Gas-Phase Ethylene Polymerization Using Zirconocene Supported on Mesoporous Molecular Sieves

P. Kumkaew,[1,2] S. E. Wanke,[1] P. Praserthdam,[2] C. Danumah,[3] S. Kaliaguine[3]

[1]*Department of Chemical and Materials Engineering, University of Alberta, Edmonton, Alberta, Canada T6G 2G6*
[2]*Department of Chemical Engineering, Chulalongkorn University, Bangkok, Thailand 10300*
[3]*Département de Génie Chimique, Université Laval, Ste-Foy, Quebec, Canada G1K 7P4*

Received 15 February 2002; accepted 18 April 2002

ABSTRACT: Mesoporous molecular sieves, with pore diameters of 2.6–25 nm, were impregnated with methylaluminoxane and bis(butylcyclopentadienyl)zirconium dichloride and tested as catalysts for the gas-phase homopolymerization of ethylene at ethylene pressures of 200 psi and temperatures of 50–100°C and for 1-hexene/ethylene copolymerization at 70°C. The activities and activity profiles, at constant Zr and Al contents, depended on the pore size of the supports and the polymerization temperature. Maximum activities for both the homopolymerizations and copolymerizations were observed for catalysts made with supports having pore diameters of 2.6 and 5.8 nm. Homopolymerization activities were highest at temperatures of 70–80°C; average homopolymerization and copolymerization activities up to 9000 kg of polyethylene/(mol of Zr h) were obtained. The weight-average molecular weights (M_w's) were not a function of the support pore size but decreased with increasing reaction temperatures, from about 260,000 at 50°C to about 165,000 at 100°C. The polydispersities were essentially constant at 2.5 ± 0.2 for the homopolymers. M_w's for the 1-hexene/ethylene copolymers had an average value of 117,000 with an average polydispersity of 2.8. The amount of triisobutyl aluminum added to the reactor significantly affected the activity and activity profiles. © 2002 Wiley Periodicals, Inc. J Appl Polym Sci 87: 1161–1177, 2003

Key words: catalysis; supports; metallocene catalysts

INTRODUCTION

Polyethylene (PE) is the most widely used synthetic polymer; world consumption exceeded 50 million tons in 2000.[1] PE has such large usage because its chemical stability and great range of physical properties make it suitable for a broad range of applications, from strong, flexible films and coatings to rigid containers. It is the variations in the molecular structure that result in this range of physical properties. Major changes have occurred in the ability to control the molecular structure in the large-scale production of ethylene since the first commercial production of PE in the 1930s.[2] A major change occurred in the 1970s when the large-scale production of linear low-density polyethylene (LLDPE) was commercialized.[3] The production of LLDPE experienced large growth rates, and it is, and continues to be, the most rapidly growing type of PE.[4,5] The newest type of PE to be commercialized is LLDPE produced with metallocenes or other single-site catalysts; the production of this type of PE, frequently denoted mLLDPE, is expected to increase by 15–20% a year in the next few years if production and processability problems are resolved.[6]

The development of supported metallocene catalysts suitable for use in gas-phase reactors, such as fluidized bed reactors, would resolve the main production problems, which are reactor fouling and the requirement of large amounts of a cocatalyst. Several reviews dealing with supported (i.e., heterogenized) single-site catalysts and the properties required for commercial applications in slurry or gas-phase reactors have appeared in recent years.[7–9] The emphasis in this article is on the use of supported metallocene catalysts in gas-phase polymerization because it is predicted that the majority of mLLDPE will be produced in gas-phase processes,[10] and very little has been published in the open literature on gas-phase polymerization over metallocene catalysts.

The majority of the ethylene polymerization studies with metallocene catalysts have been performed with homogeneous catalysts,[9] and the vast majority of the studies with supported metallocene have been performed in the slurry mode (e.g., see ref. 7). Roos et al.[11] were among the first to report detailed gas-phase ethylene polymerization results, including activity profiles, for silica-supported metallocene catalysts. Harrison et al.[12] reported high activity for gas-phase ethylene and ethylene/1-hexene polymerizations over alumina- and silica-supported metallocene catalysts, but no detailed gas-phase polymerization results were reported. Ray and coworkers[13–15] recently published

Correspondence to: S. E. Wanke (sieg.wanke@ualberta.ca).
Contract grant sponsor: Natural Sciences and Engineering Research Council of Canada.
Contract grant sponsor: Thailand Research Fund.

Journal of Applied Polymer Science, Vol. 87, 1161–1177 (2003)

TABLE I
Description of Supports

Support designation	Pore diameter (nm)	Surface area (m^2/g)	Pore volume (cm^3/g)	Crystallization temperature (°C)	Crystallization time (h)	Surfactant
MMS2.6	2.6	1130	1.3	70	168	C_{16}TABr
MMS5.8	5.8	980	0.8	62	24	P123
MMS7.2[a]	7.2	870	1.1	90	24	P123
MMS10[b]	10	412	1.3	100	48	P123
MMS15.2	15.2	330	1.3	120	48	P123
MMS20	20	310	1.6	145	48	F127
MMS25	25	300	1.7	150	72	F127
S0.54[c]	0.56	435	—			
S1[d]	16	270	1.4			

[a] 2 g of mesitylene added.
[b] 1.5 g of mesitylene added
[c] Silicalite.
[d] Silica gel.

detailed kinetic results for ethylene/propylene and ethylene/1-hexene copolymerization in the gas phase over silica/methylaluminoxane (MAO)-supported metallocene catalysts, but no details about the catalysts used and the properties of the PE produced were provided. No studies were found in the open literature that describe the relationships between the support structure, polymerization activity, and polymer properties for gas-phase ethylene polymerization with supported metallocene catalysts.

In their recent extensive review of catalytic applications of mesostructured materials, Trong On et al.[16] included a section on the use of mesoporous materials for polymerizations. Sano and coworkers[17–20] used mesoporous molecular sieves and silica gels with various pore sizes to fractionate MAO. They used the MAO left in solution as well the MAO/support solids to prepare supported Cp_2ZrCl_2 catalysts. They observed that the activities of these catalysts for ethylene and propylene polymerization were a strong function of the pore sizes of the supports used to fractionate the MAO. All the polymerization studies by Sano and coworkers[17–20] were performed with toluene slurries. The objectives of this investigation were to determine the influences of the pore sizes of supports and polymerization conditions on the gas-phase polymerization behavior of bis(butylcyclopentadienyl)zirconium dichloride ($(n\text{-BuCp})_2ZrCl_2$) supported on MAO-treated mesoporous molecular sieve silicas with pore diameters of 2.6–25 nm. Gas-phase homopolymerizations of ethylene and 1-hexene/ethylene copolymerizations were investigated.

EXPERIMENTAL

Materials

Supports

The supports used in this work are described in Table I. The mesoporous molecular sieves (identified by the prefix MMS) were synthesized and characterized at Laval University (Ste-Foy, Canada). Sample MMS2.6 was prepared as follows. A solution (solution 1) containing the inorganic precursors was prepared from a mixture of 400 g of a sodium silicate solution, 856 g of water, and 24 g of H_2SO_4. The second one (solution 2) containing the surfactant was obtained by the dispersal of 336 g of cetyltrimethylammonium bromide (C_{16}TABr; an ionic surfactant) in 1000 g of water. Then, solution 1 was added slowly to solution 2 under mechanical stirring for 3 h. The pH of the gel was then adjusted to 11 with a dilute sulfuric acid solution. The resulting gel was transferred into a nalgen bottle, in which crystallization was allowed to take place at 70°C for 168 h. The hexagonal MCM-41 type solid product was cooled to room temperature, filtered, and washed thoroughly with deionized water until a neutral pH was obtained. This solid product was then calcined at 550°C for 12 h in air.

Samples MMS5.8, MMS7.2, MMS10, MMS15.2, MMS20, and MMS25 (where the number designates the pore diameter in nanometers) were prepared according to a slight modification of the synthesis method reported by Kevan et al.[21] In a typical synthesis, the required amount of a nonionic surfactant [2 g of pluronic $EO_{20}PO_{70}EO_{20}$ (P123) or $EO_{106}PO_{70}EO_{106}$ (F127)] was dispersed in a stirred mixture containing 15 g of water and 60 g of 2*M* HCl. This homogeneous solution was kept at 40°C for 2–3 h before the addition of 4.25 g of tetraethyl orthosilicate. The gel obtained was allowed to crystallize in a round-bottom flask or in a Teflon-lined autoclave for different times and different temperatures, as reported in Table I. After crystallization, the solid product was ambient-air-cooled, filtered, washed with deionized water, and dried in air at room temperature. The dried material was calcined at 500°C for 6 h in static air to decompose the template and to obtain a white powder of MMS of the SBA-15

type. On the basis of the variations of synthesis parameters such as the crystallization time, the crystallization temperature, the nonionic surfactant nature, and the amount of mesitylene added, MMSs with different pore diameters were prepared (see Table I).

Support S0.54 was a silicalite, an essentially aluminum-free pentasil-type zeolite formerly manufactured by Union Carbide (Tarrytown, NY).[22] The silicalite used in this study was an unpelletized sample obtained from Union Carbide and used in previous studies.[23] Support S1 was a commercial silica gel. Scanning electron micrographs of supports MMS2.6, MMS5.8, MMS20, and S0.54 are shown in the top panels of Figures 1–4. Support MMS2.6 consisted of irregularly shaped particles that appeared to be agglomerates of short fibrous particles [see Fig. 1(a,b)]. Support MMS5.8 consisted of macrofibers (Figure 2a) made up of smaller short fibers [Fig. 2(b)]. The structure of supports MMS7.2 and MMS15.2 was very similar to that of MMS5.8. MMS10 had a more globular, rather than fibrous, structure but was not as agglomerated as MMS20, as shown in the top panels of Figure 3. MMS25, like MMS20, consisted of agglomerated particles, but the agglomerates had a macroporous structure. The silicalite, shown in Figure 4(a–c), consisted of loosely agglomerated 1–3-μm crystals.

Catalysts

The catalysts used in this study are described in Table II. All the catalysts, except CAT-SD, were prepared at the University of Alberta (Edmonton, Canada) by the impregnation of the supports with toluene solutions of MAO and $(n\text{-BuCp})_2ZrCl_2$. $(n\text{-BuCp})_2ZrCl_2$ and CAT-SD were donated by NOVA Chemicals Corp (Calgary, Canada). The 10 mass % MAO in a toluene solution, neat triisobutyl aluminum (TIBA), and anhydrous toluene were obtained from Aldrich (Oakville, Canada) and used without further purification. The following procedure, with Schlenk and glove-box techniques under ultra-high-purity nitrogen (from Praxair, Edmonton, Canada), was used to impregnate the supports with MAO and $(n\text{-BuCp})_2ZrCl_2$:

1. Each support was treated in flowing ultra-high-purity nitrogen at 500°C for 7 h before being placed in a 250-mL flask equipped with a stirrer and containing 10 mL of toluene and nitrogen. The amount of support placed in the flask is indicated in Table II (small amounts of MMS were used in some of the preparations, i.e., less than 1 g, because of the lack of larger quantities of these materials).
2. MAO in a 10 mass % MAO toluene solution was added dropwise to the suspended support/toluene suspension. The amount of the solution added is shown in Table II. Gas evolution was observed during the MAO addition.
3. The suspension was stirred at room temperature for 12 h.
4. The desired amount of $(n\text{-BuCp})_2ZrCl_2$ in toluene was added to the suspension.
5. The suspension was stirred at room temperature for 4 h.
6. All the toluene was removed from the flask by evacuation at room temperature. The evacuation was continued until free-flowing solids were obtained.
7. The catalysts were stored in a glove box until they were used.

The structures of the catalysts, as shown by scanning electron microscopy, were very similar to those of the starting supports (see the middle panels in Figs. 1–4). In some cases, the catalyst preparation resulted in additional agglomeration [cf. Fig. 4(a,d)].

Polymerization procedures

The previously described reactor system[24] was used for all the polymerization studies; a schematic diagram of the reactor system is shown in Figure 5. The standard procedure for the gas-phase polymerization experiments consisted of the following steps:

1. About 80 g of sodium chloride, from Fisher Scientific (Edmonton, Canada) with an average particle size of 0.5 mm, was placed in a clean, 1-L stainless steel reactor; the NaCl acted as the seedbed.
2. The reactor assembly was tested for leaks at 300 psi with nitrogen and then evacuated overnight at 90°C.
3. The reactor was cooled to the desired reaction temperature by the oil-bath temperature being lowered to about 1 or 2°C below the desired reaction temperature.
4. Ethylene was added to the reactor to a pressure of about 20 psi.
5. The desired amount of TIBA, usually 0.15 mL, was injected into the reactor, and the data acquisition system was started (the temperatures, flow rates, and reactor pressure were recorded at 10 s intervals). The ethylene flow rates, measured with a Matheson 8142 mass flow meter (East Rutherford, NJ), were used to compute the instantaneous ethylene consumption rates.
6. Ethylene was added to the reactor to a pressure of 80 psi, and the reactor was stirred for 30 min.
7. The catalyst, contained in a catalyst injection holder charged with the catalyst in the glove box, was injected into the reactor by high-pressure ethylene (i.e., dry catalyst injection).

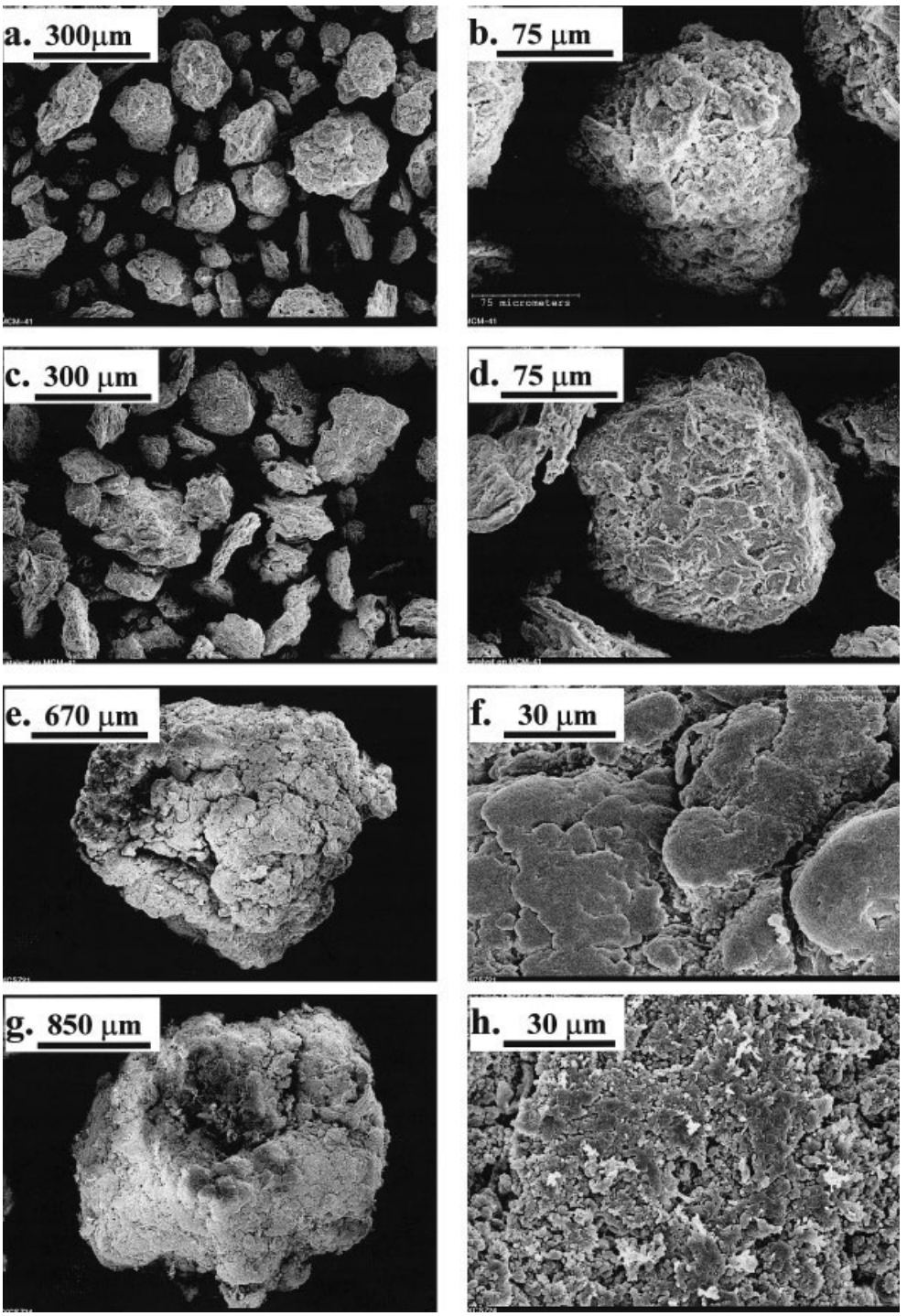

Figure 1 Scanning electron micrographs: (a,b) the MMS2.6 support, (c,d) CAT2.6-2, (e,f) the homopolymer produced with CAT2.6-2 at 70°C, and (g,h) the copolymer produced at 70°C (see Table IV for the polymerization conditions).

8. Ethylene was fed at the rate required to maintain the reactor pressure at 200 psi.
9. The polymerization was terminated after 2 h by the ethylene feed being stopped, the reactor being vented and evacuated while cooling, and the reactor then being filled with air.
10. The product was repeatedly washed with water to remove all salt, and the mass of the PE made was measured; this mass was used to calculate the average rate of polymerization.

The ethylene was polymer-grade ethylene from Matheson. It was purified by flowing through a series of three Alltech purifiers (Deerfield, IL) containing BASF R3-11, Ascarite, and 3-Å molecular sieves before entering the reactor. For gas-phase runs at a total

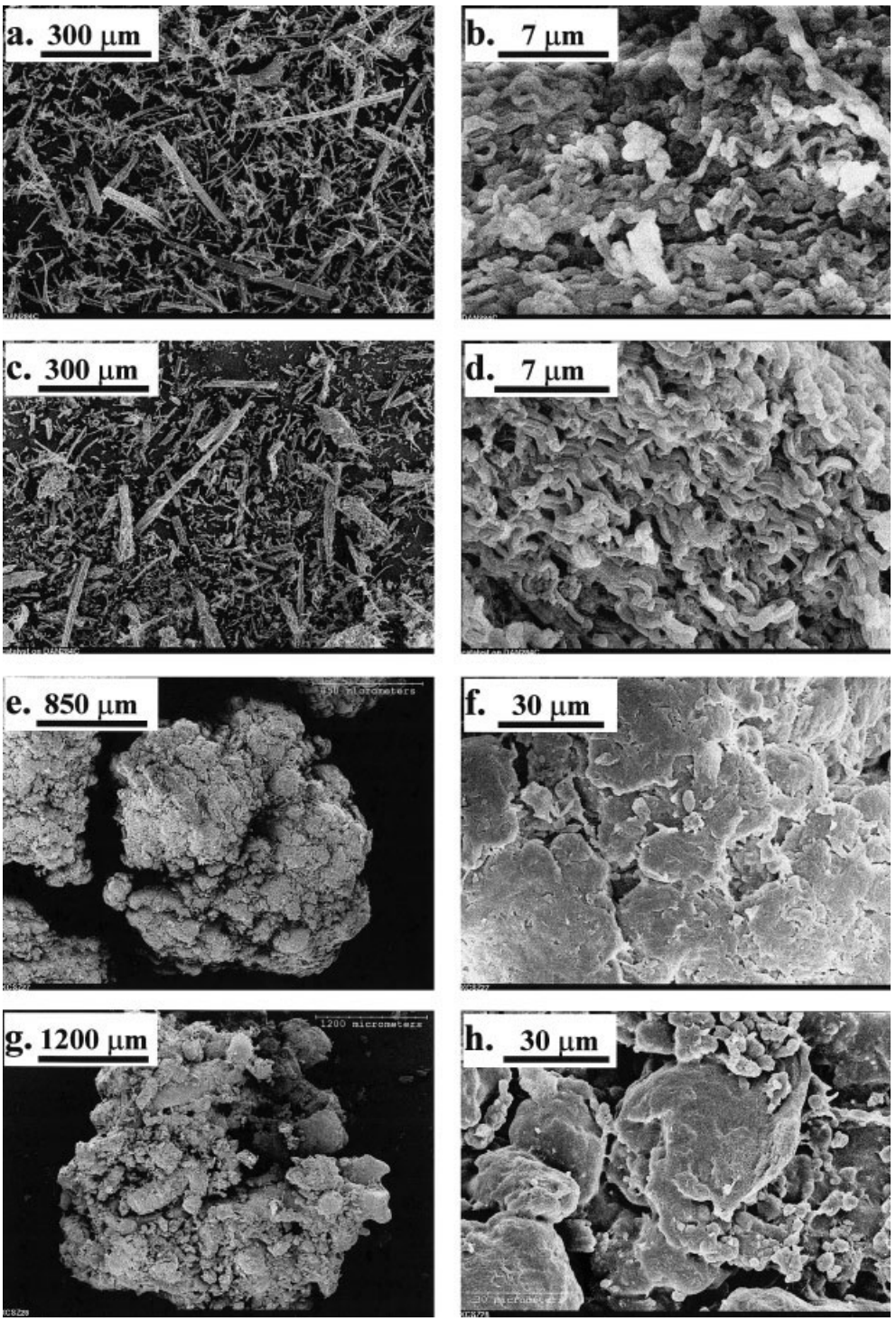

Figure 2 Scanning electron micrographs: (a,b) the MMS5.8 support, (c,d) CAT5.8, (e,f) the homopolymer produced with CAT5.8 at 70°C, and (g,h) the copolymer produced at 70°C (see Table IV for the polymerization conditions).

ethylene pressure of 100 psi, no ethylene was added in step 6; that is, the stirring for 30 min was done at a total pressure of 20 psi. For copolymerization runs, 3.2–3.5 mL of 1-hexene were injected after step 4. No seed bed was used for the slurry runs (step 1), and 300 mL of heptane was added to the reactor after the reactor had been cooled to the reaction temperature; MAO in toluene was added, ethylene was added to a pressure of 20 psi, and the catalyst suspended in heptane was added with a syringe. The reactor pressure was then increased and maintained at the desired value by the continuous addition of ethylene.

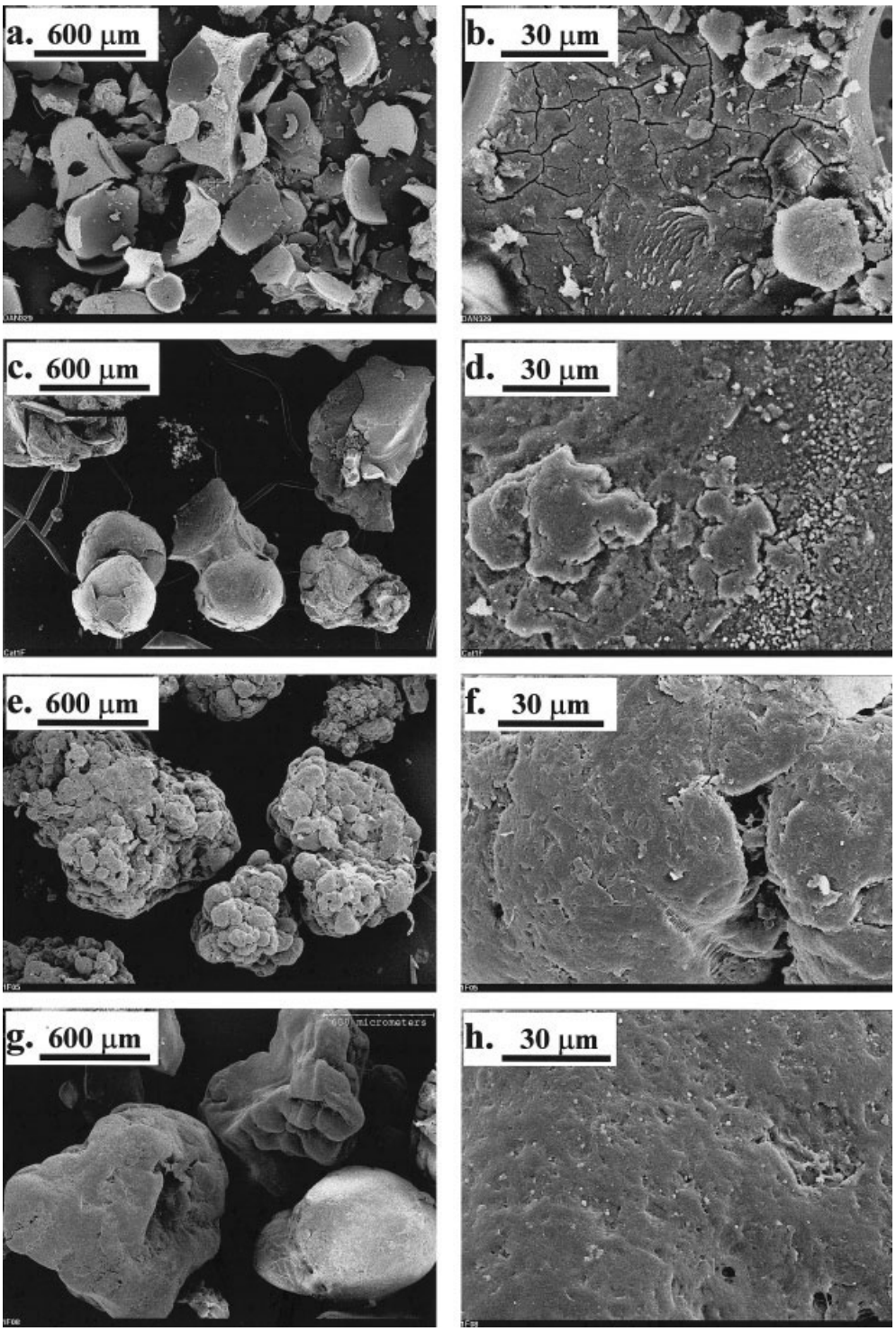

Figure 3 Scanning electron micrographs: (a,b) the MMS20 support, (c,d) CAT20, (e,f) the homopolymer produced with CAT20 at 70°C, and (g,h) the copolymer produced at 70°C (see Table IV for the polymerization conditions).

Characterization methods

The support surface areas were obtained from nitrogen sorption measurements at 77 K with an Omnisorp 100 sorptometer (Miami Lakes, FL); the Brunauer, Emmett and Teller (BET) method was used to calculate the surface area. The pore size distribution was obtained from the desorption branch of the N_2 physisorption isotherm (with the Barrett–Joyner–Halenda formula). Before each adsorption experiment, the calcined samples (MMS) were outgassed at 573 K for at least 2 h in vacuo. The surface area of the silicalite was based on a single-point BET measurement. Pore sizes

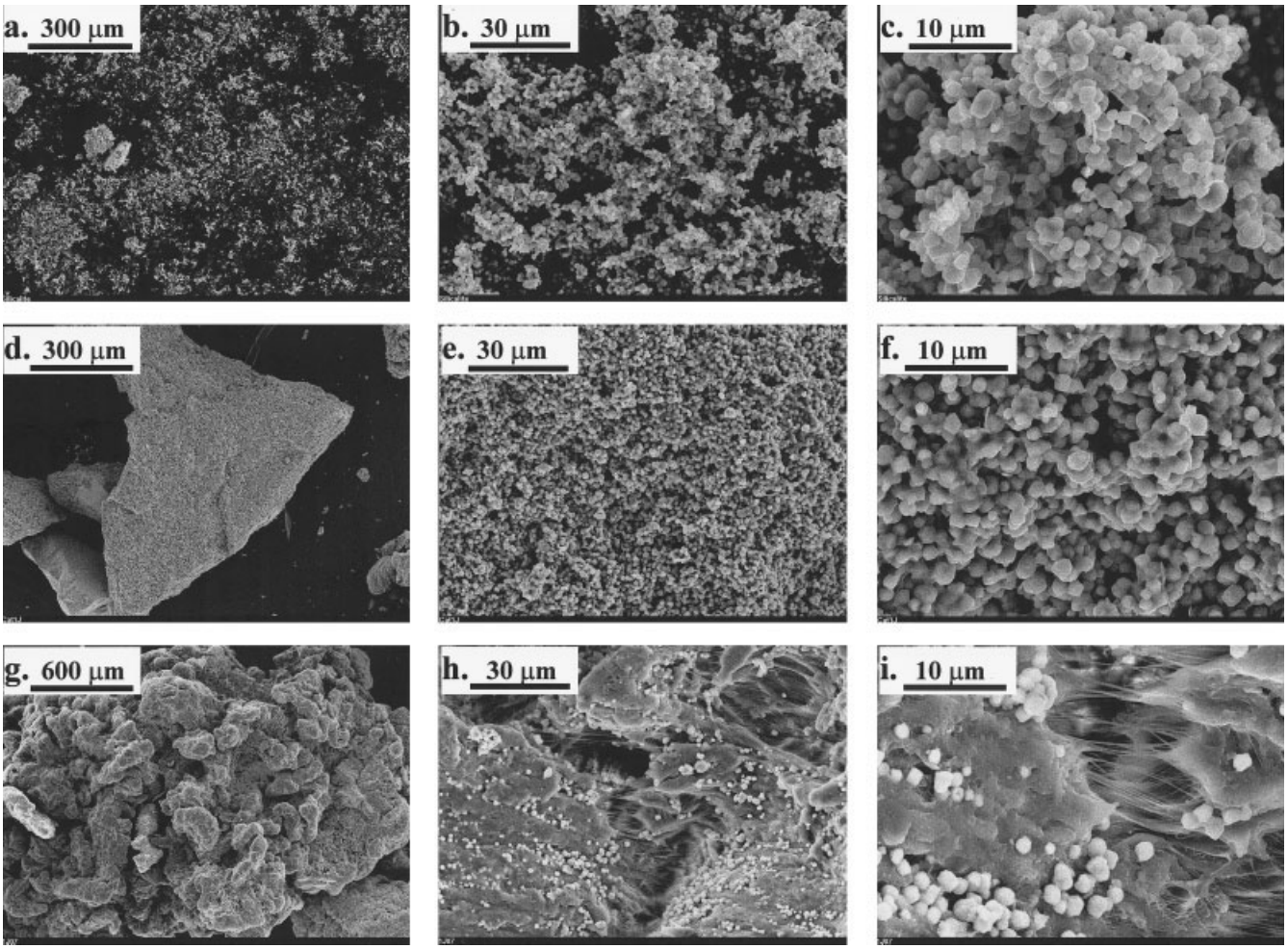

Figure 4 Scanning electron micrographs: (a–c) the S0.54 support, (d–f) CAT0.54, and (g–i) the homopolymer produced with CAT0.54 at 100°C (see Table IV for the polymerization conditions).

and pore volumes were obtained from nitrogen desorption curves. A Hitachi S-2700 scanning electron microscope was used to obtain the micrographs with digital recording of the images. Molar masses were determined with an Alliance GPCV2000 equipped with three HTGE columns from Waters corp. (Milford, MA). The columns and the detector were operated at 145°C, and high performance liquid chromatography-grade 1,2,4-trichlorobenzene (from Fisher Scientific), containing 0.25 g/L 2,6-*tert*-butyl-4-methylphenol,

TABLE II
Description of Catalysts

Catalyst	Support pore diameter (nm)	Support	Amount of support used (g)	Amount of MAO added (mL)	Zr content		Al/Zr ratio
					Mass %	mmol/g	
CAT0.54	0.54	S0.54	0.66	4.4	0.33	0.037	170
CAT2.6-1	2.6	MMS2.6	1.00	6.6	0.34	0.037	170
CAT2.6-2	2.6	MMS2.6	1.00	6.6	0.38	0.042	150
CAT2.6-3	2.6	MMS2.6	1.00	3.3	0.36	0.039	100
CAT5.8	5.8	MMS5.8	0.60	4.0	0.34	0.037	170
CAT7.2	7.2	MMS7.2	0.52	3.4	0.33	0.037	170
CAT10	10	MSP10	0.33	4.2	0.25	0.027	330
CAT15	15	MMS15	0.29	1.9	0.34	0.037	170
CAT20	20	MMS20	0.75	5.0	0.34	0.037	170
CAT25	25	MMS25	0.25	1.6	0.34	0.037	170
CATS1-1	16	S1	2.00	6.6	0.33	0.036	110
CATS1-2	16	S1	2.00	13.3	0.29	0.032	200
CAT-SD	A donated, uncharacterized (n-BuCp)$_2$ZrCl$_2$/MAO/SiO$_2$ catalyst used in preliminary experiments						

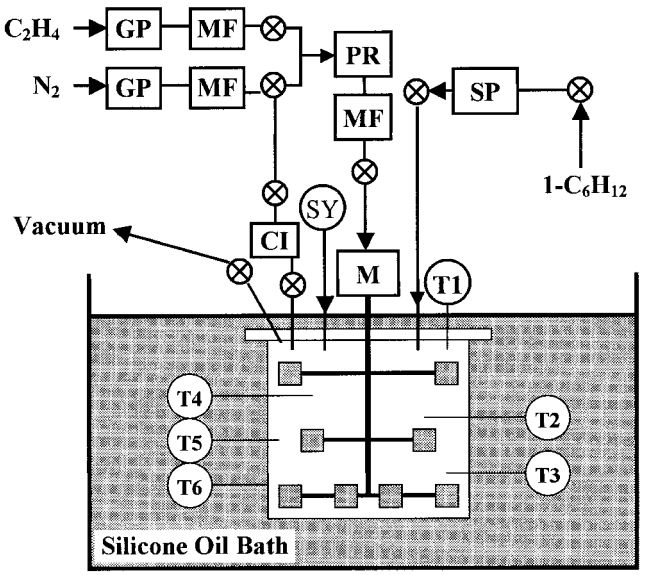

Figure 5 Schematic diagram of the reactor system: CI = catalyst injector, GP = gas purifiers, M = magnet-driven stirrer, MF = mass flow meters, PR = pressure regulator, SP = syringe pump, SY = syringe injection port, and T# = thermocouples.

was pumped through the columns at a rate of 1.0 cm^3/min. Repeat analyses were done on all samples, and the reported values are the averages of two or more analyses. Polystyrene, alkanes, and PE standards were used for molar mass calibration, as described previously.[25] The reported values are linear PE equivalent molar masses.

RESULTS AND DISCUSSION

Preliminary experiments

A number of preliminary experiments were done to determine suitable reactor conditions for gas-phase operation, to compare gas-phase activities with slurry activities, and to determine suitable Al/Zr ratios for the catalysts. The first set of experiments was performed with the catalyst CAT-SD to determine the nature of the activity profiles for the homopolymerization and copolymerization and the effect of the amount of TIBA on the polymerization activity. To minimize increases in bulk gas-phase temperatures due to the exothermic nature of the polymerization, we used small quantities of the catalyst in these experiments. The conditions for the experiments are described in Table III, and activity profiles are shown in Figure 6. The bulk gas-phase temperature increases of 3.4°C were observed for run 2, the run with the highest activity; for other runs, the bulk gas-phase temperature increases were less than 2°C. The maximum rates listed in Table III were calculated from the measured ethylene feed rates, and they are an indication of whether rises in the bulk temperature exceeding 1 or 2°C are likely. Experience with our reactor has shown that significant increases in the bulk gas-phase temperature occur if the instantaneous ethylene polymerization rate exceeds 25–30 g of ethylene per hour.

From the results presented in Table III and Figure 6, it can be concluded that the amount of TIBA has a significant effect on the activity and activity pro-

TABLE III
Results from the Preliminary Experiments

		Amounts Charged to Reactor			C_2H_4		Activity (g of PE/g of cat h)	
Catalyst	Run	Catalyst (mg)	TIBA (mmol)	1-Hexene (mL)	pressure (psi)	Temperature (°C)	Average	Maximum
CAT-SD	1	20	0.20	0	200	90	101	421
	2	20	0.40	0	200	90	464	2230
	3	20	0.60	0	200	90	451	1250
	4	10	0.20	1.42	200	90	145	410
	5	10	0.40	1.69	200	90	698	1240
CATS1-1	6	54	0.60	0	200	90	37	89
	7	53	1.00	0	200	90	22	35
	8	54	1.00	0	200	90	15	24
CATS1-2	9	53	0.60	0	200	50	20	—
CAT2.6-1	10	51	0.60	0	200	50	184	223
	11	52	0.60	0	200	70	377	761
CAT2.6-2	12	50	0.60	0	200	70	210	524
CAT2.6-3	13	50	0.60	0	200	70	60	—
CATS1-2	14	55	*[a]	0	200	50	347	—
CAT2.6-3	15	50	*[a]	0	100	50	481	—
CAT2.6-2	16	51	0.60	0	100	80	92	247
	17	50	0.60	0	200	80	241	880
CAT5.8	18	50	0.60	0	100	80	170	490
	19	54	0.60	0	200	80	293	556

[a] Slurry runs: no TIBA was added, but 14 mmol of Al as MAO was added to the slurry.

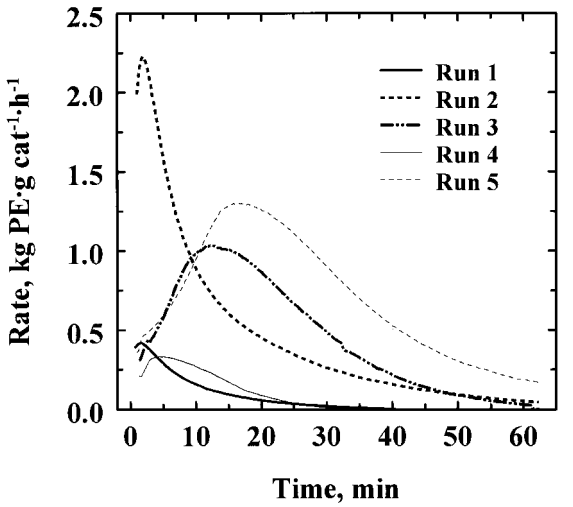

Figure 6 Activity profiles for CATS1 (see Table III for the polymerization conditions).

file; too little TIBA resulted in low activities (cf. run 1 with run 2 and run 4 with run 5); larger amounts of TIBA resulted in decreases in activity (cf. runs 2 and 3). The low activities observed when only 0.2 mmol of TIBA was used (runs 1 and 4) were probably due to incomplete scavenging of the impurities resulting in the subsequent deactivation of some of the catalyst. The amount of TIBA also has a marked effect on the shape of the activity profiles; larger amounts of TIBA broaden the activity profile with a decrease in the maximum activity; however, the average activity did not change significantly (cf. runs 2 and 3). The activity profile for copolymerization was also broad (run 4), similar to that for the homopolymerization with 0.6 mmol of TIBA. The comonomer effect, that is, activity enhancement due to the presence of a comonomer commonly observed for copolymerizations,[26] was also observed for CAT-SD (cf. average rates for runs 2 and 5).

Britto et al.[26] investigated the effect of the TIBA concentration during 1-hexene/ethylene copolymerization in a hexane slurry with a homogeneous $Et(Ind)_2ZrCl_2$–MAO/TIBA catalyst; they observed increases in the polymerization activity and amount of 1-hexene incorporation as the amount of TIBA was increased. They attributed the activity increase to an increase in MAO solubility in hexane with increasing TIBA concentrations. No studies on the effect of TIBA during gas-phase polymerizations were found in the open literature; such studies should be done because the aforementioned results indicate that TIBA plays a more complex role during gas-phase polymerization over supported metallocene catalysts than simply being a scavenger of impurities.

A silica gel-supported catalyst (CATS1-1) with an Al/Zr ratio of 110 was prepared according to the procedure described previously and tested for activity (run 6 in Table III); the activity was low, and increasing the amount of TIBA (runs 7 and 8) did not improve the activity. However, the increased amounts of TIBA resulted in a large delay in the activation of the catalyst (see Fig. 7). Another silica gel-supported catalyst (CATS1-2) with an Al/Zr ratio of 200 and an MMS2.6-supported catalyst (CAT2.6-1) with an Al/Zr ratio of 170 were prepared. The gas-phase polymerization activity for CATS1-2 was also low (run 9 in Table III), but the activity of CAT2.6-1 was relatively high (run 10). Two more MMS2.6-supported catalysts were prepared (CAT2.6-2, Al/Zr = 150, and CAT2.6-3, Al/Zr = 100) to determine whether the Al/Zr ratio had a large effect on the activity. The results for runs 11–13 (Table III) show that the activity was sensitive to the Al/Zr ratio; the activity increased by a factor of 3.5 when the Al/Zr ratio was increased from 100 to 150, and an additional increase of about 80% occurred with an increase in the Al/Zr ratio from 150 to 170. On the basis of these observations, it was decided that all other catalyst preparations would have Al/Zr ratios of at least 170.

Slurry runs were done to confirm that the low Al/Zr ratio was the reason for the low activities of CATS1-2 and CAT2.6-3 (runs 14 and 15); the Al/Zr ratio was increased to 8800 for run 14 and to 7000 for run 15 by the addition of MAO to the heptane. The activities for these slurry runs were much higher than the gas-phase activities; a greater than 15-fold increase in the activity occurred for CATS1-2 (cf. runs 9 and 14). The activity profiles for the slurry runs were also markedly different than the gas-phase activity profiles (see Fig. 8). The typical gas-phase activity profiles had an initial period of increasing activity followed by a decay in activity; the activity profiles for the slurry phase did not display deactivation behavior.

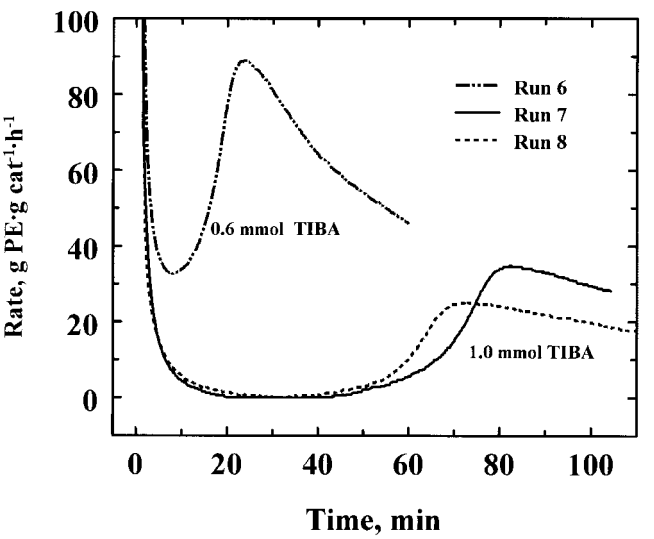

Figure 7 Effect of the amount of TIBA on the activity profile.

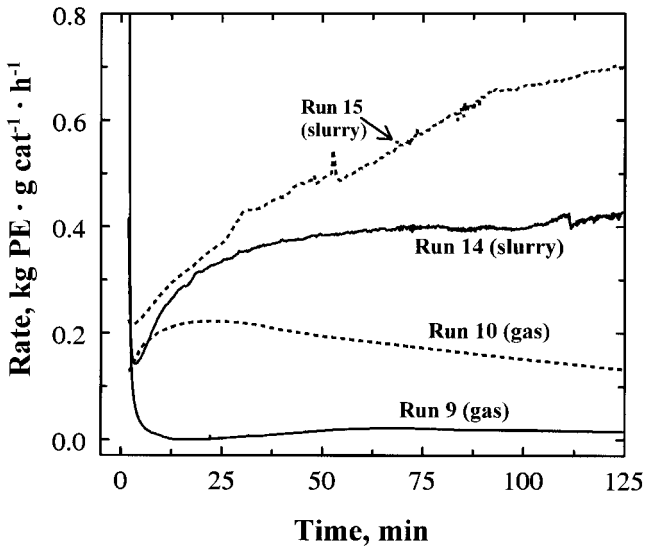

Figure 8 Comparison of the gas-phase and slurry activity profiles (see Table III for the conditions).

Finally, four experiments (runs 16–19) were performed to determine the effect of ethylene pressure on the polymerization rates (runs 16–19 in Table III). Doubling the ethylene pressure from 100 to 200 psi increased the average rates by a factor of 2.6 and 1.7 for catalysts CAT2.6-2 and CAT5.8, respectively. It is not expected that the average rates vary linearly with the gas-phase monomer concentration because the activity profiles for these catalysts, shown in Figure 9, have different activation–deactivation characteristics. The activity profile for run 19 shows a delay in the activation similar to, but not as pronounced as, that observed for cases in which higher amounts of TIBA were used (see runs 7 and 8 in Fig. 7). Therefore, it is likely that the concentration of TIBA was higher for run 19 than for run 18, possibly because of the lower consumption of TIBA for scavenging impurities. If overall polymerization rates for these types of hybrid activity profiles, such as those in Figure 9, are fit by power-law functions, an overall order between 1 and 2 usually results.[25] At the end of the runs, that is, after 2 h of polymerization, the ratios of instantaneous specific polymerization rates for runs at 200 psi of ethylene pressure to those at 100 psi were 2.2 and 2.4 for catalysts CAT2.6-2 and CAT5.8, respectively. It is likely that these ratios would approach 2.0, that is, first-order kinetics, at longer polymerization times when activation and deactivation rates are expected to become slow; for run 19, the pseudo-steady state was not achieved after 2 h of reaction time (see Fig. 9). It seems that the specific activity during the pseudo-steady state (at long reaction times) becomes relatively independent of the initial activation–deactivation behavior.

Homopolymerization results

The homopolymerization activities for the various MMS-supported and silicalite-supported catalysts were measured at an ethylene pressure of 200 psi and at temperatures of 50–100°C. The average activities are summarized in Table IV; these results show that the average polymerization rates were a function of the temperature and pore diameter of the support. Catalysts made with supports MMS2.6 and MMS5.8 had the maximum average rates; supports with larger pores yielded catalysts with lower activities, and the catalyst made with the small-pore silicalite had the lowest homopolymerization activities at all temperatures. The dependence of the activity on the pore size of the MMS supports appeared to decrease as the polymerization temperature increased, that is, at 100°C, the variation in the average activities was a factor of three, whereas the activities at 90, 80, 70, and 50°C varied by factors of about 4, 5, 6, and 7, respectively (catalysts CAT2.6-1 and CAT25 are not included in this comparison because their activities were not measured at all the temperatures). The dependencies of the average rate on the pore diameter at 80 and 100°C are illustrated in Figure 10. The variations in the activities with the support type cannot be attributed to variations in the support surface areas or support pore volumes (see Table II) because no trends in activity as a function of the support surface area or pore volume could be detected.

The observed trends in activity as a function of the support pore size were very similar to those observed by Sano et al.[17,18] for the slurry polymerization of ethylene with Cp_2ZrCl_2 supported on various silylated mesoporous molecular sieves, silica gels, and silicalite that had been soaked in an MAO toluene

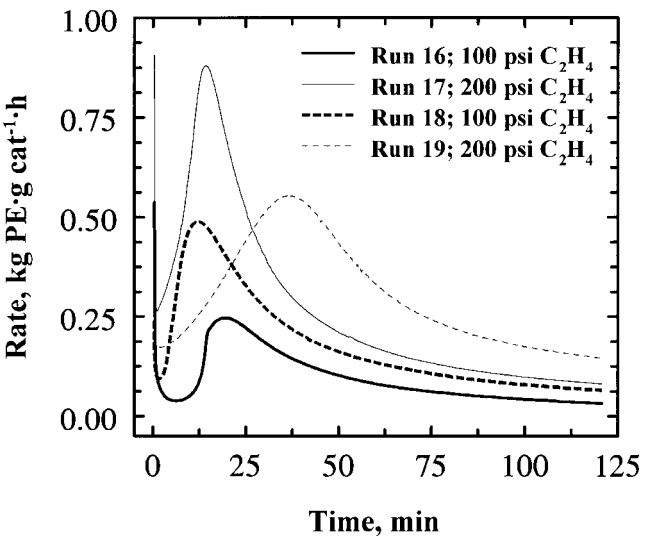

Figure 9 Effect of the ethylene pressure on the activity profiles.

TABLE IV
Average Ethylene Polymerization Activities as Functions of Temperature and Support

Catalyst	Support pore diameter (nm)	Al/Zr ratio	Average polymerization activities (g of PE/g of cat h)					
			50°C	70°C		80°C	90°C	100°C
				Homopolymerization	Copolymerization[a]			
CAT0.54	0.54	170	8	6	56	22	5	3
CAT2.6-1	2.6	170	249	339	330	—	—	—
CAT2.6-2	2.6	150	107	210	324	241	206	125
CAT5.8	5.8	170	47	172	136	293	137	152
CAT7.2	7.2	170	91	200	34	165	92	111
CAT10	10	330	141	186	0	208	156	98
CAT15	15	170	103	181	6	168	111	66
CAT20	20	170	19	37	63	61	55	52
CAT25	25	170	—	53	—	60	56	—

(Reaction conditions: ethylene pressure = 200 psi; amount of catalyst = 52 (±2) mg; amount of TIBA = 0.6 mmol; Polymerization time = 2h).

[a] 3.2–3.4 mL of 1-hexene was added at the beginning of each copolymerization run.

solution. The preparation techniques used by Sano and coworkers[17–20] fractionated the MAO in the toluene solution, and the MAO left in the toluene yielded catalysts with different activities than the MAO retained by the supports. In our catalyst preparation techniques, no macroscopic fractionation of the MAO occurred because all the MAO in the toluene was deposited onto or into the support (all the toluene was evaporated). However, some fractionation of the MAO must have occurred within the support particles; otherwise, it is difficult to explain the activity dependence on the support pore diameter.

MAO consists of a mixture of linear and cyclic oligomers of trimethylaluminum, which exist in dynamic equilibrium.[27] It has been proposed that the MAO species responsible for activating metallocenes consist of a cyclic cage structure made from CH_3AlO units.[27,28] The higher activity of the catalysts made with MMS having pore diameters of 2.6 and 5.8 nm can be explained if we assume that the active MAO species are preferentially adsorbed by the MMS with small pores or possibly even stabilized by interaction with the surfaces of the small pores, such as a shift in the equilibrium from linear MAO to cyclic MAO. In larger pores, such segregation of MAO or favored formation of active MAO would not occur; it is even possible that the absorption or formation of linear forms of MAO may be favored by some pore sizes. MAO cannot enter the very small pores of the silicalite-supported catalyst (CAT0.54), and this is the reason for its very low activity. Sano et al.[17,18] also observed very low activities for silicalite-supported catalysts.

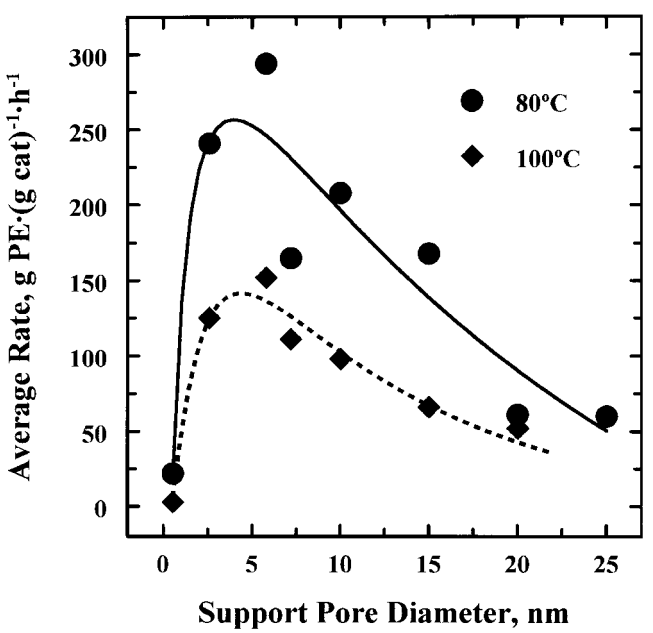

Figure 10 Effect of the support pore diameter on the average homopolymerization activity.

The pore size of the supports also had a significant effect on the shapes of the activity profiles; this is illustrated in Figures 11–13. All activity profiles showed a period of activation followed by deactivation, but the rates of activation and deactivation were functions not only of the temperature but also of the support pore diameter. Deactivation rates were more sensitive to temperature than activation rates; that is, there was a higher activation energy for the deactivation process(es) than for the activation process(es) of the catalytic sites. This behavior is well illustrated in Figure 11. The top panels in Figures 11–13 show the changes in the bulk gas-phase temperature as indicated by the average value measured with thermocouples T3 and T5 (Fig. 5); the temperature increases at these locations were the highest because they were located where most of the reaction occurred. The tip of thermocouple T6 was located very close to the inside surface of the reactor wall and provided an indication of the in-

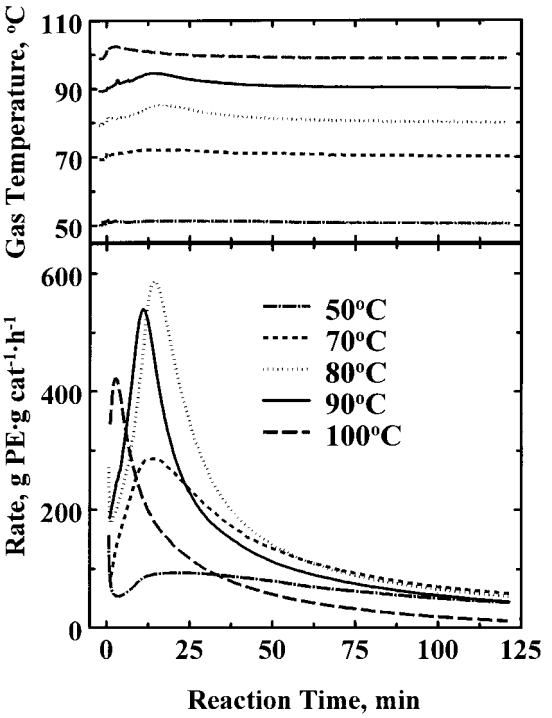

Figure 11 Activity and temperature profiles as a function of the reaction temperature for CAT2.6-2.

side wall temperature rather than the gas-phase temperature.

The activity profiles for CAT5.8 (Fig. 12) were broader than those for CAT2.6-2, but the average activities for the two catalysts were about the same. The difference in the activity profiles for these two catalysts may be due to the size and shape of the catalyst (support) particles. CAT2.6-2 consisted of chunky 100–300-μm particles [see Fig. 1(a–d)], whereas CAT5.8 consisted of fibrous particles with diameters of about 20–50 μm. Therefore, temperature gradients inside the growing catalyst/polymer particles are likely to be larger for CAT2.6-2 than for CAT5.8, especially during the initial high-activity period. Temperatures inside the catalyst/polymer particles may be considerably higher than the bulk gas-phase temperature; such temperature gradients would lead to rapid activation followed by rapid deactivation, that is, profiles of the type observed for CAT2.6-2 (Fig. 11). The activity profiles for CAT20, shown in Figure 13, are broad, and there is no measurable increase in the bulk gas-phase temperature because of the low activity of this catalyst. Therefore, it is unlikely that there were significant differences between gas-phase and catalyst-particle temperatures even though the catalyst particles were relatively large (see Fig. 3). These observations indicate that the initial catalyst particle size as well as the support pore diameters can significantly affect the activity profiles.

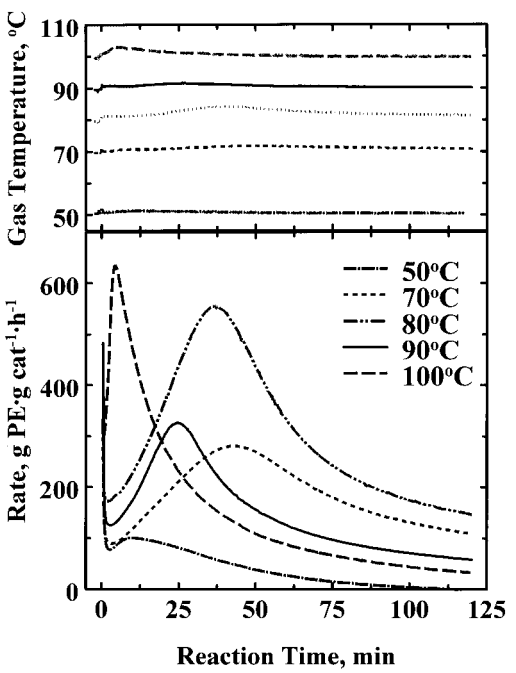

Figure 12 Activity and temperature profiles as a function of the reaction temperature for CAT5.8.

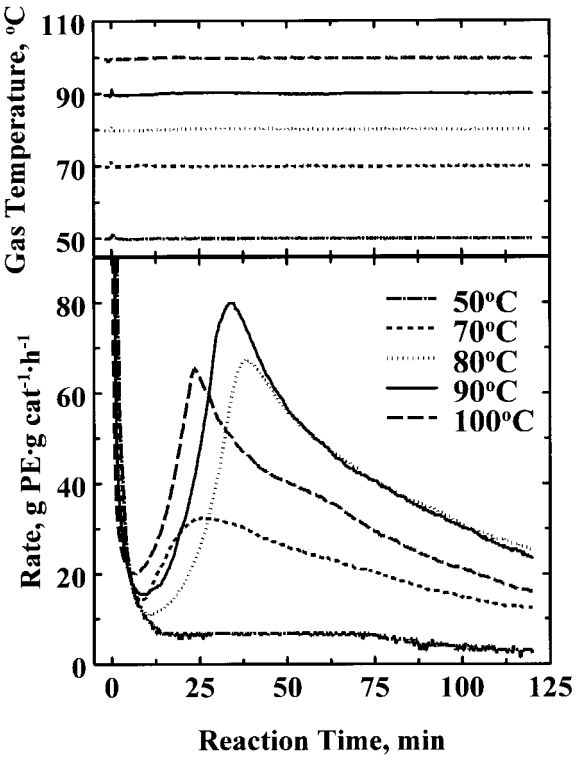

Figure 13 Activity and temperature profiles as a function of the reaction temperature for CAT20.

Copolymerization results

Copolymerization activities for 1-hexene/ethylene were measured at 70°C. 1-Hexene was injected only at the beginning of each copolymerization run; that is,

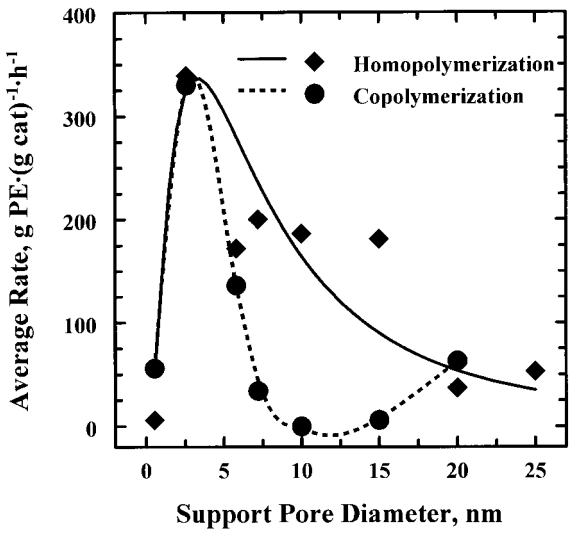

Figure 14 Comparison of the effects of the support pore diameter on the average homopolymerization and copolymerization activities at 70°C.

the 1-hexene concentration was varied throughout the run. The amount of liquid 1-hexene injected into the reactor at the beginning of each copolymerization run was 3.3 ± 0.1 mL. The initial 1-hexene partial pressure for 3.4 mL of 1-hexene was about 11 psi; the vapor pressure of 1-hexene at 70°C was 18 psi. The average copolymerization activities, listed in Table IV, were much more support-dependent than the homopolymerization activities. The copolymerization and homopolymerization activities at 70°C are compared in Figure 14. The copolymerization activities of catalysts made with support pore diameters of 7.2–15 nm were very low, even though the homopolymerization activities were quite high. The reason for this unusual behavior is unknown. Unfortunately, insufficient amounts of the catalyst were available for repeat measurements; however, it is unlikely that all three copolymerization experiments with the catalysts made with the larger pore sizes were in error.

The activity profiles for the copolymerizations are shown in Figure 15. All the profiles are broad, even those for the high-activity catalysts (CAT2.6-1 and CAT2.6-2). This indicates that the 1-hexene participated in the site activation processes, but the reasons for the very marked difference in the homopolymerization and copolymerization activity profiles are not known. The degree of 1-hexene incorporation has not yet been determined, but the presence of 1-hexene does have a significant effect on the molar masses, as discussed later. Additional copolymerization experiments with freshly prepared catalysts and the characterization of the polymers, including the determination of 1-hexene incorporation, are required to obtain more insight into the copolymerization processes over mesoporous molecular sieve-supported $(n\text{-BuCp})_2ZrCl_2$ catalysts.

Polymer properties

Information on the morphology of the polymers produced was obtained by scanning electron microscopy, and representative micrographs of the polymers produced are shown in the bottom panels of Figures 1–4. The homopolymer particles made with MMS-supported catalysts all consisted of agglomerates of fairly dense, platelike polymer particles. The fiber morphology of CAT5.8, CAT7.2, and CAT15 was not replicated into the polymer particle morphology. The morphology of the polymer made with CAT0.54 (silicalite-supported) was different than that of the polymers made with MMS-supported catalysts (bottom panels of Figs. 1–4). The structure of the polymer made with CAT0.54 was more open, and unfractured silicalite particles are clearly visible in the polymer matrix [Fig. 4(h,i)]; that is, MAO and $(n\text{-BuCp})_2ZrCl_2$ did not enter the pores of the silicalite, and MAO and $(n\text{-BuCp})_2ZrCl_2$ in CAT0.54 were supported on the external surface of the silicalite crystals, similar to the catalyst prepared by Goretzki et al.,[29] except that the silicalite particles were much smaller than the silica gel particles that they used.

The structures of the copolymer particles made with CAT2.6-2 and CAT5.8 were more porous [see Figs. 1(h) and 2(h)] than those of the homopolymers. The micrograph for a copolymer made with CAT20 [Fig. 3(h)] does not show a porous structure, but other regions of the particles shown in Figure 3(g) are porous. The region shown in Figure 3(h) was chosen because it clearly shows unfractured catalyst (support) particles. This indicates that some of the support particles were not active, possibly because of a lack of impregnation with MAO and/or $(n\text{-BuCp})_2ZrCl_2$; this may be the reason for the low copolymerization activity of CAT20.

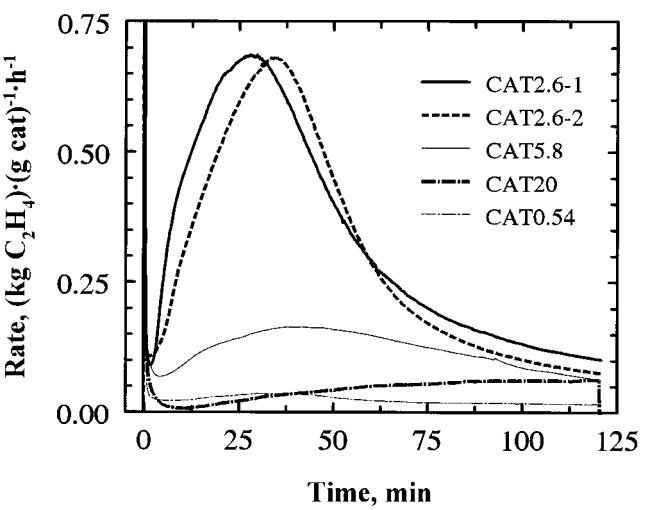

Figure 15 Activity profiles for 1-hexene/ethylene copolymerization with various catalysts.

TABLE V
Parameter Values for Molar Mass Correlations [eqs. (1) and (2)]

Catalyst	Parameters for M_n			Parameters for M_w		
	a_n	b_n	r^2	a_w	b_w	r^2
CAT2.6-2	7.469	1330	0.95	7.773	1546	0.98
CAT5.8	8.523	987	0.55	9.035	1121	0.68
CAT7.2	7.958	1200	0.86	8.957	1154	0.95
CAT10	8.875	845	0.91	10.034	748	0.91
CAT15	7.901	1216	0.96	8.966	1160	0.99
CAT20	8.359	963	0.95	8.806	1179	0.95
CAT0.54	6.176	1609	0.65	10.080	630	0.52

Molar masses were measured for most of the products, and it was found that the dependence of the molar masses on the polymerization temperatures was reasonably well correlated by eqs. (1) and (2):

$$\ln(M_n) = a_n + \frac{b_n}{T} \quad (1)$$

$$\ln(M_w) = a_w + \frac{b_w}{T} \quad (2)$$

Equation (1) would be the expected correlation for the number-average molecular weight (M_n) as a function of temperature if transfer to monomer was the main-chain termination reaction. The values of the constants a_n, b_n, a_w, and b_w, as well as the correlation coefficients r^2, for the various catalysts for which products were obtained at four or more temperatures are listed in Table V. Plots illustrating the best fit (CAT15) and the worst fit (CAT5.8) for polymers made with mesoporous molecular sieve-supported catalysts are shown in Figure 16. The lines for the polydispersities in Figure 16 are given by the ratios of eqs. (1) and (2), and the data points are based on the ratios of the measured weight-average molecular weight (M_w) and M_n values. The polydispersities for all the MMS-supported catalysts were essentially independent of temperature, with values of 2.3–2.7 for all catalysts except CAT20, for which the polydispersities varied from 2.7 to 3.1.

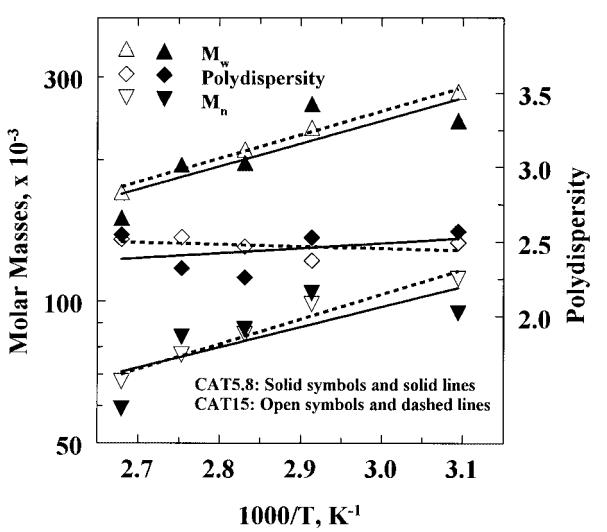

Figure 16 Sample plots of molar mass/temperature correlations.

The molar masses for all catalysts decreased with increasing polymerization temperature, indicating that the overall activation energies for the propagation reactions were lower than those for the chain termination reactions. On the basis of the values of b_n in Table V, the difference in the average values of the lumped termination and propagation activation energies, that is, $E_{\text{termination}} - E_{\text{propagation}}$, is 9.1 kJ/mol; $E_{\text{termination}} - E_{\text{propagation}}$, on the basis of b_w, is 9.6 kJ/mol. The average ratio of the lumped pre-exponential factors for propagation steps to termination steps, according to a_n values, is 3570. The molar masses for MMS-supported catalysts were relatively independent of the type of catalyst; this indicates that the nature of the active sites was relatively independent of the pore sizes of the mesoporous molecular sieves. The molar masses of the polymers made with CAT0.54 were lower than those made with MMS-supported catalysts, and the polydispersity of polymers made with CAT0.54 increased with increasing temperature (see the correlation values in Table V). Therefore, the nature of the sites in the silicalite-supported catalyst (CAT054), in which neither MAO nor $(n\text{-BuCp})_2ZrCl_2$ entered the pores, was different than those of the MMS-supported catalysts.

The molar masses for 1-hexene copolymers were lower than those of homopolymers made at similar temperatures and ethylene pressures; the copolymer and homopolymer molar masses are compared in Figure 17. The molar masses for the polymers made with CAT0.54 are not included in the trend lines shown in Figure 17 because the molar masses for both the homopolymer and copolymer made with CAT0.54 were much lower than those of polymers made with MMS-supported silicas. The polydispersity of the copolymer made with CAT0.54 was 7.1,

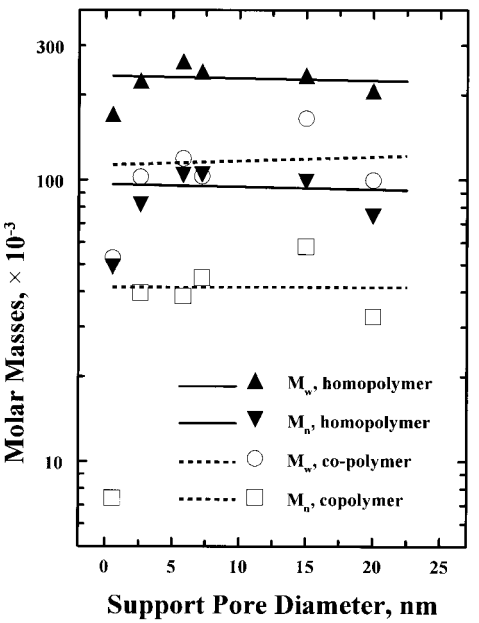

Figure 17 Molar masses for homopolymers and copolymers made at 70°C with catalysts of different pore sizes.

indicating the presence of multiple types of catalytic sites in this catalyst.

The molar masses of homopolymers made at 100 psi of ethylene pressure (runs 16 and 18 in Table III) were lower than the molar masses of homopolymers made with the same catalysts at 200 psi of ethylene pressure (runs 17 and 19 in Table III). For CAT2.6-2, M_w decreased from 180×10^3 to 150×10^3, and for CAT5.8, M_w decreased from 187×10^3 to 153×10^3 with a decrease in the ethylene pressure from 200 to 100 psi. The polydispersities for polymers made at 100 psi of ethylene pressure were 2.7, whereas the polydispersities were 2.4 and 2.3 for polymers made at 200 psi with CAT2.6-1 and CAT5.8, respectively. The dependence of the molar masses on the ethylene pressure indicates that chain termination by modes other than transfer to monomer occurred. Molar masses would be essentially independent of ethylene pressure for the case in which chain transfer to monomer is the main mode of chain termination if the common assumption holds that both propagation and transfer-to-monomer rates are first-order in the monomer.[34]

Comparison of the activity profiles and activities with those in the literature

Activity profiles are only reported infrequently in the literature, and activity profiles for gas-phase polymerization over supported metallocene catalysts are even rarer. Only two studies that reported gas-phase activity profiles for ethylene polymerization were found in the literature: the 1997 study by Roos et al.[11] and the recent study by Ray and coworkers.[13–15] Roos et al. used 1 mass % $Me_2Si[Ind]_2ZrCl_2$ on an MAO-treated silica as a catalyst, and Ray and coworkers used bridged and unbridged metallocenes supported on MAO-containing silicas; the nature of the metallocenes was not specified. The activity profiles in both of these studies had similar shapes to those reported in this study, that is, an activation period followed by deactivation. The activation was very rapid in the study by Roos et al., and some oscillations were apparent in the ethylene feed rates in the initial 30 min of the runs because of temperature control.

The average normalized gas-phase polymerization activity at 70°C (i.e., activity per mole of Zr and per atmosphere of ethylene pressure) of the supported $Me_2Si[Ind]_2ZrCl_2$ catalyst used by Roos et al.[11] was essentially the same as that of CAT2.6-2 used in this work. In Table VI, these average gas-phase activities are compared to some average activities obtained for slurry operations. Comparisons are made with slurry results because normalized activities, other than the study by Roos et al., are not available in the open literature for gas-phase studies with supported metallocene catalysts. Comparing activities, even normalized average activities, should be done with care because different polymerization conditions have been used by various investigators. In the absence of activity profiles, which is frequently the case, it is impossible to know whether the average activity for a short polymerization time is comparable to that for a longer polymerization time; therefore, the normalization of activities to a time period of 1 h can be very misleading. Despite these difficulties, it is possible to draw the following general conclusions from the results in Table VI: first, the average activities of silica-supported metallocenes in slurries are up to 10-fold higher than average gas-phase activities if the Al/Zr ratio is increased by the addition of MAO to the slurry, and second, if no additional MAO is added to the slurry, then gas-phase and slurry activities appear to be approximately equal. Increases in gas-phase activities for supported metallocene catalysts may be attainable by the support surface being changed to improve interactions with MAO.[12]

CONCLUSIONS

The aforementioned results have shown that gas-phase ethylene polymerization activities and activity profiles of $(n\text{-BuCp})_2ZrCl_2$ supported on mesoporous molecular sieves are functions of the pore size of the mesoporous molecular sieves. The highest activity catalysts were those prepared with supports having pore diameters of 2.6 and 5.8 nm. All the gas-phase activity profiles had an initial activation period followed by deactivation, and the deactivation was more temperature-sensitive than the activation. Therefore, overheating of the catalyst/polymer particles during the initial stages of polymerization could cause rapid catalyst deactivation. The

TABLE VI
Comparison of Average Polymerization Rates Over Silica-Supported Metallocene Catalysts

Catalyst	Support	Reactor mode	Al/Zr Ratio[a]	Temperature (°C)	Pressure of C_2H_4 (psi)	Normalized rate[b]	Comments	Reference
(n-BuCp)$_2$ZrCl$_2$	MMS/MAO	Gas	150	70	200	420	CAT2.6-2	[c]
(n-BuCp)$_2$ZrCl$_2$	MMS/MAO	Gas	150	70	200	640	1-C_6H_{12} copolymerization	[c]
Me_2[Ind]$_2$ZrCl$_2$	Silica/MAO	Gas	383	70	73	440		11
(n-BuCp)$_2$ZrCl$_2$	Silica/trimethyl aluminum	Slurry	—	70	560	63	Hydrated silica treated with TMA	30
(n-BuCp)$_2$ZrCl$_2$	Silica/MAO	Slurry	326	20	30	400	Activity from activity profile	29
(n-BuCp)$_2$ZrCl$_2$	Silica	Slurry	3000	70	15	510	No Al added to SiO_2	31
en[Ind]$_2$ZrCl$_2$	Silica/MAO	Slurry	1000	20	60	2,250	Added MAO to slurry	12
Cp$_2$ZrCl$_2$	MMS/MAO	Slurry	40	20	60	200	Activity after 10 min	16
Cp$_2$ZrCl$_2$	Silica/MAO	Slurry	1000	60	145	370	Added MAO to slurry	27
Cp$_2$ZrCl$_2$	MMS/MAO	Slurry	2000	50	36	2,240	Added MAO to slurry	32
Cp$_2$ZrCl$_2$	Silica/MAO	Slurry	2000	50	36	4,000	Added MAO to slurry	32
Cp$_2$ZrCl$_2$	Silica/MAO	Slurry	2757	70	15	5,000	Added MAO to slurry	33

[a] The Al/Zr ratio includes Al added to the catalyst and Al added to the slurry.
[b] Normalized rate kg of PE/(mol of Zr h atm of C_2H_4).
[c] This work.

MMS-supported catalysts were also active for 1-hexene/ethylene copolymerization. Molar masses decreased with increasing polymerization temperature, but the polydispersities were essentially independent of the polymerization temperature; the average value of the polydispersity was 2.5. The molar masses and polydispersities were not functions of the MMS support pore size. The activity and activity profiles were very strong functions of the amount of TIBA added; increases in the amounts of TIBA resulted in slower activation and broader activity profiles.

The dependence of the gas-phase ethylene polymerization activity on the support pore size should provide guidance for the development of more active supported metallocene catalysts for ethylene homopolymerization and copolymerization. The marked effect of the TIBA concentration on the activity profiles is useful for the optimization of reactor conditions for improved productivity and operating stability.

The authors thank N. Bu for the molar mass measurements and J. Zhou for the preliminary experiments with the catalyst CAT-SD.

References

1. Robinson, S. Chem Ind 2001, 12, 377.
2. Bett, K. E.; Crossland, R.; Ford, H.; Gardner, A. K. In Polyethylenes 1933–83, Proceedings of the Golden Jubilee Conference, The Plastics and Rubber Institute, London, 1983; p B1.1.
3. Staub, R. B. In Polyethylenes 1933–83, Proceedings of the Golden Jubilee Conference, The Plastics and Rubber Institute, London, 1983; p B5.4.1.
4. Phillip Townsend Assoc Newslett Plast Chem Ind 2001, 56.
5. Buckalew, L.; Schumacher, J. W. Chem Econ Handb SRI Int Plast Resins 2000, 580.1321.
6. Chem Ind Newslett SRI Consult 2000, No. 3, 1.
7. Ribeiro, M. R.; Deffieux, A.; Portela, M. F. Ind Eng Chem Res 1997, 36, 1224.
8. Chien, J. C. W. Top Catal 1999, 7, 23.
9. Hlatky, G. G. Chem Rev 2000, 100, 1347.
10. Foxley, D. Chem Ind 1998, 8, 305.
11. Roos, P.; Meier, G. B.; Samson, J. J. C.; Weickert, G. Macromol Rapid Commun 1997, 18, 319.
12. Harrison, D.; Coulter, I. M.; Wang, S.; Nistala, S.; Kuntz, B. A.; Pigeon, M.; Tian, J.; Collins, S. J. Mol Catal A 1998, 128, 65.
13. Xu, Z. G.; Chakravarti, S.; Ray, W. H. J Appl Polym Sci 2001, 80, 81.
14. Chakravarti, S.; Ray, W. H. J Appl Polym Sci 2001, 80, 1096.
15. Xu, Z. G.; Chakravarti, S.; Ray, W. H.; Zhang, S. X. J Appl Polym Sci 2001, 81, 1451.
16. Trong On, D.; Desplantier-Giscard, D.; Danumah, C.; Kaliaguine, S. Appl Catal A 2001, 222, 299.
17. Sano, T.; Doi, K.; Hagimoto, H.; Wang, Z.; Uozumi, T.; Soga, K. Chem Commun 1999, 733.
18. Sano, T.; Doi, K.; Hagimoto, H.; Wang, Z.; Uozumi, T.; Soga, K. Stud Surf Sci Catal 1999, 125, 777.
19. Sano, T.; Hagimoto, H.; Jin, J.; Oumi, Y.; Uozumi, T.; Soga, K. Macromol Rapid Commun 2000, 21, 1191.
20. Sano, T.; Hagimoto, H.; Sumiya, S.; Naito, Y.; Oumi, Y.; Uozumi, T.; Soga, K. Microporous Mesoporous Mater 2001, 44, 557.
21. Luan, Z.; Maes, E. M.; van der Heide, P. A. W.; Zhao, D.; Czernuszewicz, R. S.; Kevan, L. Chem Mater 1999, 11, 3680.

22. Flanigen, E. M.; Bennet, J. M.; Grose, R. W.; Cohen, J. P.; Patton, R. L.; Kirchner, R. M.; Smith, J. V. Nature 1978, 271, 512.
23. Rangwala, H. A.; Szymura, J. A.; Wanke, S. E.; Otto, F. D. Can J Chem Eng 1988, 66, 843.
24. Lynch, D. T.; Wanke, S. E. Can J Chem Eng 1991, 69, 332.
25. Wu, L.; Lynch, D. T.; Wanke, S. E. Macromolecules 1999, 32, 7990.
26. Britto, M. L.; Galland, G. B.; dos Santos, J. H. Z.; Forte, M. C. Polymer 2001, 42, 6355.
27. Alt, H. G.; Köppl, A. Chem Rev 2000, 100, 1205.
28. Sinn, H. Macromol Symp 1995, 97, 27.
29. Goretzki, R.; Fink, G.; Tesche, B.; Steinmetz, B.; Rieger, R. J. J Polym Sci Part A: Polym Chem 1999, 37, 677.
30. Lee, D.; Shin, S. Macromol Symp 1995, 97, 195.
31. dos Santos, J. H. Z.; Krug, C.; da Rosa, M. B.; Stedile, F. C.; Dupont, J.; de C. Forte, M. J. Mol Catal A 1999, 139, 199.
32. Rahiala, H.; Beurroies, I.; Eklund, T.; Hakala, K.; Gougeon, R.; Trens, P.; Rosenholm, J. B. J Catal 1999, 188, 14.
33. Tait, P. J. T.; Monteiro, M. G. K. Polimery 2000, 45, 314.
34. Kissin, Y. V. Isospecific Polymerization of Olefins; Springer-Verlag: New York, 1985.